Edge Detection in Gravity Field of the Gheshm Sedimentary Basin

Seyed Ali Akbar Hosseini[1*], Faramarz Doulati Ardejani[2], Seyed Hashem Tabatabaie[3], Ardeshir Hezarkhani[4]

[1] Department of Mining Engineering, Science and Research Branch, Islamic Azad University, Tehran, Iran

[2] Faculty of Mining, Petroleum and Geophysics, Shahrood University of Technology, Shahrood Iran

[3] P.O.Box: 36155-316, Shahrood, Iran.Exploration Division, National Iranian Oil Company, Tehran, Iran

[4] Faculty of Mining and Metallurgical Engineering, Amirkabir University of Technology, Iran

Abstract

Edge detection and edge enhancement techniques play an essential role in interpreting potential field data. This paper describes the application of various edge detection techniques to gravity data in order to delineate the edges of subsurface structures. The edge detection methods comprise analytic signal, total horizontal derivative (THDR), theta angle, tilt angle, hyperbolic of tilt angle (HTA), normalised total horizontal gradient (TDX) and normalised horizontal derivative (NTHD). The results showed that almost all filters delineated edges of anomalies successfully. However, the capability of these filters in edge detection decreased as the depth of sources increased. Of the edge enhancement filters, normalized standard deviation filter provided much better results in delineating deeper sources. The edge detection techniques were further applied on a real gravity data from the Gheshm sedimentary basin in the Persian Gulf in Iran. All filters specified a northeast-southwest structural trend. The THDR better outlined the structural morphology and trend. Moreover, it indicated the salt plugs much better than other filters. Analytic signal and THDR successfully enhanced the edges of the shorter wavelength residual structures. Normalized standard deviation (NSTD), TDX and hyperbolic of tilt angle (HTA) filters highlighted the likely fault pattern and lineaments, with a dominant northeast-southwest structural trend. This case study shows that the edge detection techniques provides valuable information for geologists and petroleum engineers to outline the horizontal location of geological sources including salt plugs and stand out buried faults, contacts and other tectonic and geological features.

1. Introduction

The lateral location of the edges of contributing sources is an essential component in interpreting potential field data. The edge detection filters are often used to enhance the edges of anomalies and make them more visible [1]. So many filters have been proposed by many researchers to perform this task [2]. Most of these methods are based on horizontal and vertical derivatives of potential field data [3, 4].

Cordell and Grauch proposed a method for the position of the horizontal extents of the causative bodies from the maxima of the horizontal gradient of the pseudo-gravity resulted in the magnetic data [5]. However, one of the most important disadvantages of derivative-based edge detection and enhancement techniques is that the noise in the potential filed data increases during the process. Hansen et al. applied the horizontal gradient and the analytic signal on gravity data to delineate edges and dips [6]. Thurston and Smithi used vertical derivative as an effective tool to delineate edges in gravity and magnetic field data [7]. Boschetti employed gravity gradients to improve edge detection process and remove noise in gravity maps [8]. Wijns *et al.* introduced a theta map filter to detect edge in magnetic data [9]. Fedi *et al.* applied two-dimensional continuous wavelet transform on potential field data to study extended geological

sources [10]. Oruç used the tilt angle map (TAM) obtained from the first vertical gradient of gravity data of the Kozakl-Central Anatolia Region, Turkey, to detect edges and estimate depth of gravity anomalies [11]. Oruç and Selim applied the tilt derivative (TDR), Euler deconvolution (ED) and discrete wavelet transform (DWT) on total field magnetic anomaly data to enhance magnetic anomalies and identify structural lineaments in the Sinop area of mid Black Sea, northern Turkey [1]. They determined the source boundaries from the zero contours of magnetic data.

Applying structure tensor technique on gravity and magnetic data, Sertcelik and Kafadar [9] extracted the edges and corners of causative bodies using eigenvalue analysis of structure tensor. In contrast to traditional edge detection techniques, the structure tensor was successful in reducing noise in the potential field data while enhancing discontinuity boundaries. Ma and Li presented normalised horizontal derivative (NTHD) as an edge detection technique for potential filed data [13]. The NTHD filter was computed from the ratio of the horizontal derivative to the maxima of nearby values. Comparison between the results of NTHD and those obtained by the conventional edge detection techniques based on the horizontal and vertical derivatives showed that the proposed method could make the strong and weak amplitudes of source edges visible simultaneously.

The main objective of this research was to apply different edge detection techniques on gravity data to identify possible faults, structural trend and the edges of salt plugs in the Gheshm sedimentary basin, Persian Gulf, Iran. The edge detection methods include analytic signal, total horizontal derivative of tilt angle (THDR-TA), NSTD, THDR, theta angle, tilt angle, TDX and HTA. Most of these methods agree closely in identifying the structural trend and horizontal locations of salt plugs and other causative sources. We first analysed synthetic gravity sources, trying to signify real-world geological sources, and then applied the methods to a real case.

2. Edge detection filters
The edge detection filters used in this study to delineate the edges of sources are summarised in Table 1. These filters were calculated as the functions of vertical and horizontal derivatives of potential filed data.

Table 1. Edge detection techniques used in this study

No	Filter	Equation	Reference
1	Tilt angle	$TA = \tan^{-1}\left[\dfrac{\delta f / \delta z}{\sqrt{(\delta f / \delta x)^2 + (\delta f / \delta y)^2}}\right]$	Miller and Singh [4]
2	Total horizontal derivative of tilt angle	$THDR\text{-}TA = \sqrt{(\delta TA / \delta X)^2 + (\delta TA / \delta Y)^2}$	Verduzco et al. [14]
3	Theta angle	$\cos\theta = \left[\dfrac{\sqrt{(\delta f / \delta x)^2 + (\delta f / \delta y)^2}}{\sqrt{(\delta f / \delta x)^2 + (\delta f / \delta y)^2 + (\delta f / \delta z)^2}}\right]$	Wijns et al. [9]
4	Analytic signal	$|A| = \sqrt{(\delta f / \delta x)^2 + (\delta f / \delta y)^2 + (\delta f / \delta z)^2}$	Nabighian [15]
5	Hyperbolic of tilt angle	$HTA = R\left[\tanh^{-1}\left[\dfrac{\delta f / \delta z}{\sqrt{(\delta f / \delta x)^2 + (\delta f / \delta y)^2}}\right]\right]$	Cooper and Cowan [16]
6	Total horizontal derivative	$TDX = \sqrt{(\delta f / \delta x)^2 + (\delta f / \delta y)^2}$	Cooper and Cowan [16]
7	Normalised horizontal derivative	$NTHD = \tan^{-1}\left(\dfrac{\sqrt{(\delta f / \delta x)^2 + (\delta f / \delta y)^2}}{|\delta f / \delta z|}\right)$	Ma and Li [13]

TA= Tilt angle, f = Gravity or magnetic field, $\partial f / \partial x, \partial f / \partial y, \partial f / \partial z$ = First derivatives of the field f in the x, y and z directions, THDR-TA= Total horizontal derivative of tilt angle, $\cos\theta$ = Theta filter, $|A|$ = Analytic signal, HTA= Hyperbolic of tilt angle, R= Real component of the function (potential field), TDX= Total horizontal derivative, NTHD= Normalised horizontal derivative

3. Synthetic gravity anomaly

Figure 1a shows a model comprising two geological bodies. The depths to the tops of the two bodies are 2km (left body) and 3km (right body), respectively. Both bodies are defined with a density contrast of 1000 kg/m^3. Figure 1b demonstrates the gravity anomaly due to this model. Figure 1c illustrates the tilt angle of gravity data. And Figure 1d shows the total horizontal derivative (THDR). Theta filter, vertical derivative, analytic signal, NTHD and HTA of gravity data are shown in Figures 1e through 1i, respectively. The tilt angle is maximum and positive at the center of bodies (Figure 1c). It is zero at the edges of bodies and negative outside the source regions. However, this filter is not sensitive to the depth of the gravity sources. THDR effectively enhanced the source edges at different depths. The peak of this filter is on the edges of bodies (Figure 1d). THDR is minimum at the bodies centre. However, the edge detection resolution decreased as causative body's depth increased. Since the THDR has been calculated from the second derivatives of the tilt angle, some noises may be added to the result. The maximum values of the theta map delineate the spatial location of the edges of the models (Figure 1e). The theta

filter is effective in defining the edges, even if the models are located at different depths.

The horizontal location of the models is at the position where the vertical derivative has the zero value (Figure 1f). A maximum value of 12 mgal/km is shown at the center of the body with lower depth to the top of the body whereas the vertical derivative is about 9 mgal/km at the centre of the deeper body, suggesting that an increase in the depth of the gravity source decreased the vertical derivative value. The edges of the shallower body show a good resolution.

The analytic signal of gravity anomaly of the synthetic model is shown in Figure 1g. The edges of bodies have been enhanced; however, the edges of the deeper body cannot be recognised clearly.

As shown in Figure 1h, the maxima of the NTHD filter are located on the edges of causative bodies. It is clear that the NTHD of the gravity anomaly can delineate the edges of the bodies more clearly, even at different depths.

Figure 1i shows the HTA of the gravity anomaly of the synthetic model. It is evident that the HTA filter can enhance the source edges effectively. However, the detected edges are not in close agreement with the actual edges.
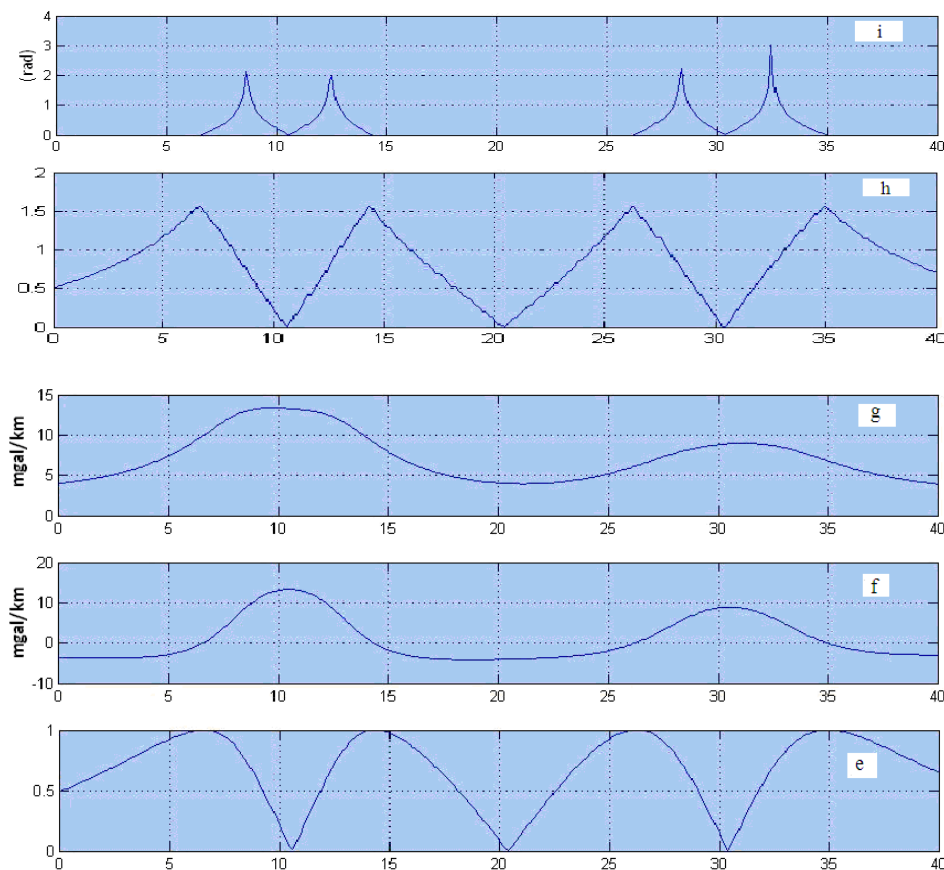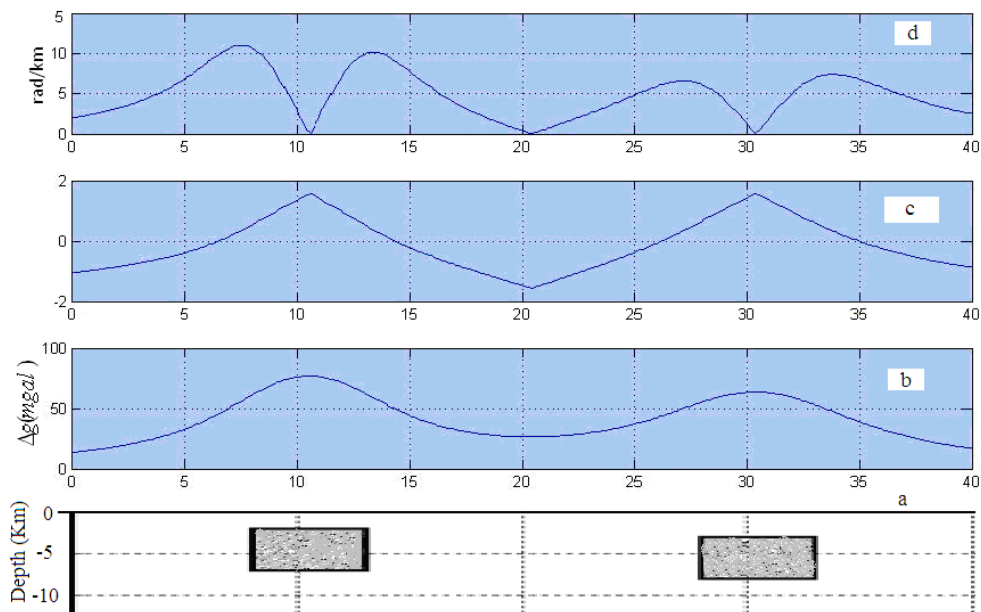
Figure 1. a) Geologic model, b) Gravity anomaly, c) Tilt angle of data, d) THDR of data, e) Theta map, f) Vertical derivative, g) Analytic signal of data, h) NTHD of data, i) HTA of data (Modified from Hadadian [17])

Figure 2a shows a plan view of a synthetic model including two vertical quadrangles, and Figure 2b and Figure 2c show the plan view and horizontal section of the associated gravity anomaly. Figure 2d illustrates the analytic signal of gravity anomaly. Figure 2e shows the first vertical derivative of analytic signal and Figure 2f shows the second vertical derivative of analytic signal. Figure 2g depicts the normalized standard deviation and Figure 2h shows the tilt angle of data. Figure 2i illustrates the hyperbolic of tilt angle. The total horizontal derivative, total horizontal derivative of tilt angle, theta angle, normalised total horizontal gradient, normalized first vertical derivative of total horizontal derivative and the normalized second vertical derivative of total horizontal derivative are shown in Figure 2j through Figure 2o, respectively.

The capability of the local phase filters to detect deep sources decreased. To overcome some of the limitations of the existing filters, the application of the filters based on the derivative of local phase filters provides better response and they act as effective tool to delineate edges in gravity field data. It is evident that the normalized standard deviation filter provides the best separation. Higher orders vertical derivatives make the interpretation more complicated, due to noise generation problem.

Figure 3a shows the plan view of the gravity anomaly of a synthetic model including three vertical cubics. Figure 3b through Figure 3l shows the results of various edge detection filters. The edge detection methods include: Analytic signal (Figure 3b), theta angle (Figure 3c), total horizontal derivative of tilt angle (Figure 3d), total horizontal derivative (Figure 3e), tilt angle (Figure 3f), normalized standard deviation (Figure 3g), normalised total horizontal gradient (Figure 3h), normalised first vertical derivative of total horizontal derivative (Figure 3i), hyperbolic of tilt angle (Figure 3j), vertical derivative (Figure 3k) and first vertical derivative of analytic signal (Figure 3l) respectively.

The results indicate that almost all filters delineated the edges of anomalies successfully. However, the capability of these filters for edge detection decreases as the depth of sources increases. Of the local phase filters, normalized standard deviation filter (Figure 3g) provides much better results in delineating deeper sources.

Application of edge detection techniques to real gravity data

This section considers the application of edge detection methods to real gravity data from the Gheshm sedimentary basin in the Persian Gulf. The study area was located in the seashore and shallow waters from east of the Gheshm Island and its northern seashores from the Sarkhun to Latidan, with an area of 12000 km^2 (Figure 4).
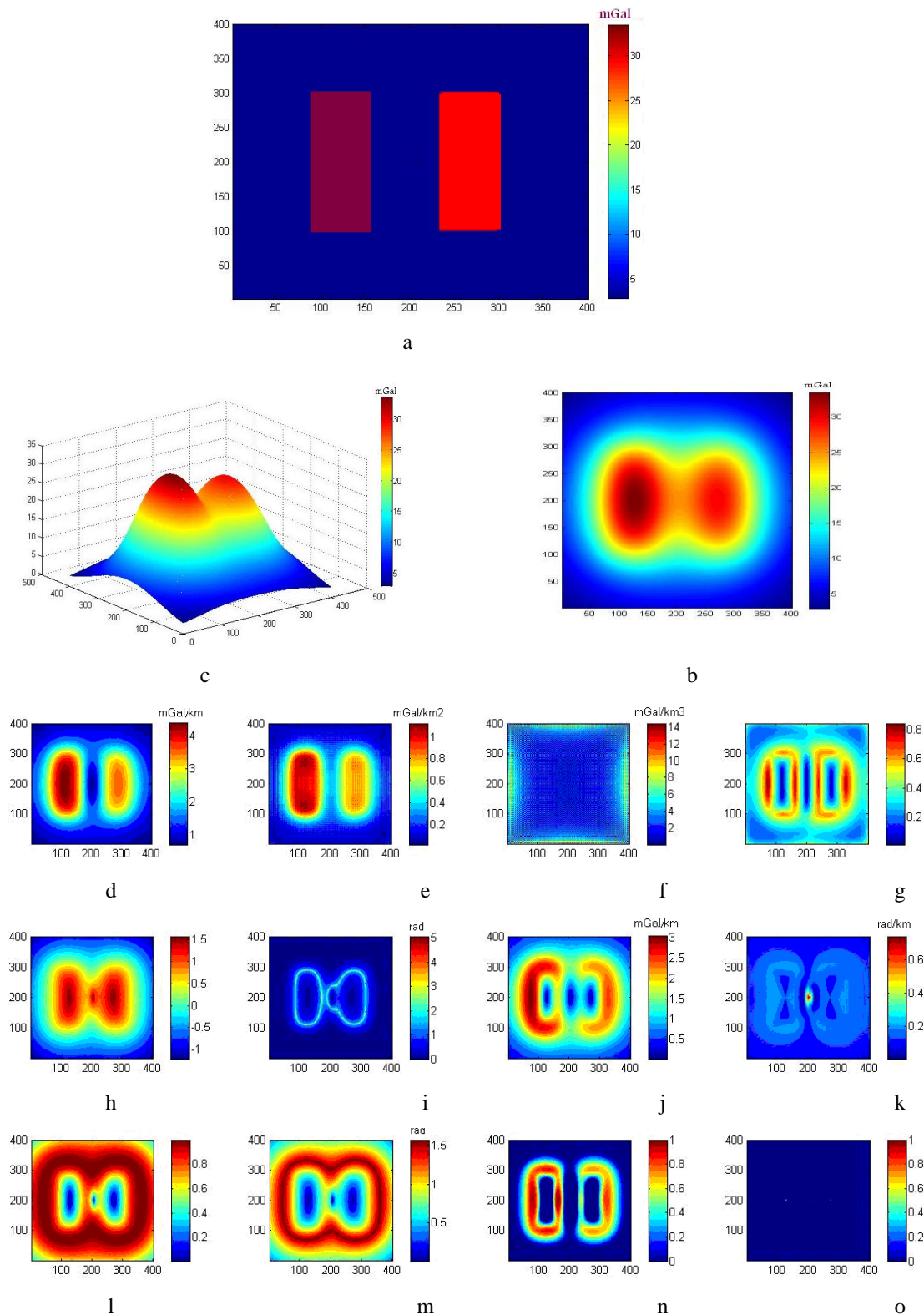
Figure 2. a) Plan view of a synthetic model including two vertical quadrangles, b) Plan view of gravity anomaly, c) Horizontal section of the gravity anomaly, d) Analytic signal, e) First vertical derivative of analytic signal, f) Second vertical derivative of analytic signal, g) Normalized standard deviation, h) Tilt angle, i) Hyperbolic of tilt angle, j) Total horizontal derivative, k) Total horizontal derivative of tilt angle, l) Theta angle, m) Normalised total horizontal gradient, n) Normalised first vertical derivative of total horizontal derivative, o) Normalised second vertical derivative of total horizontal derivative
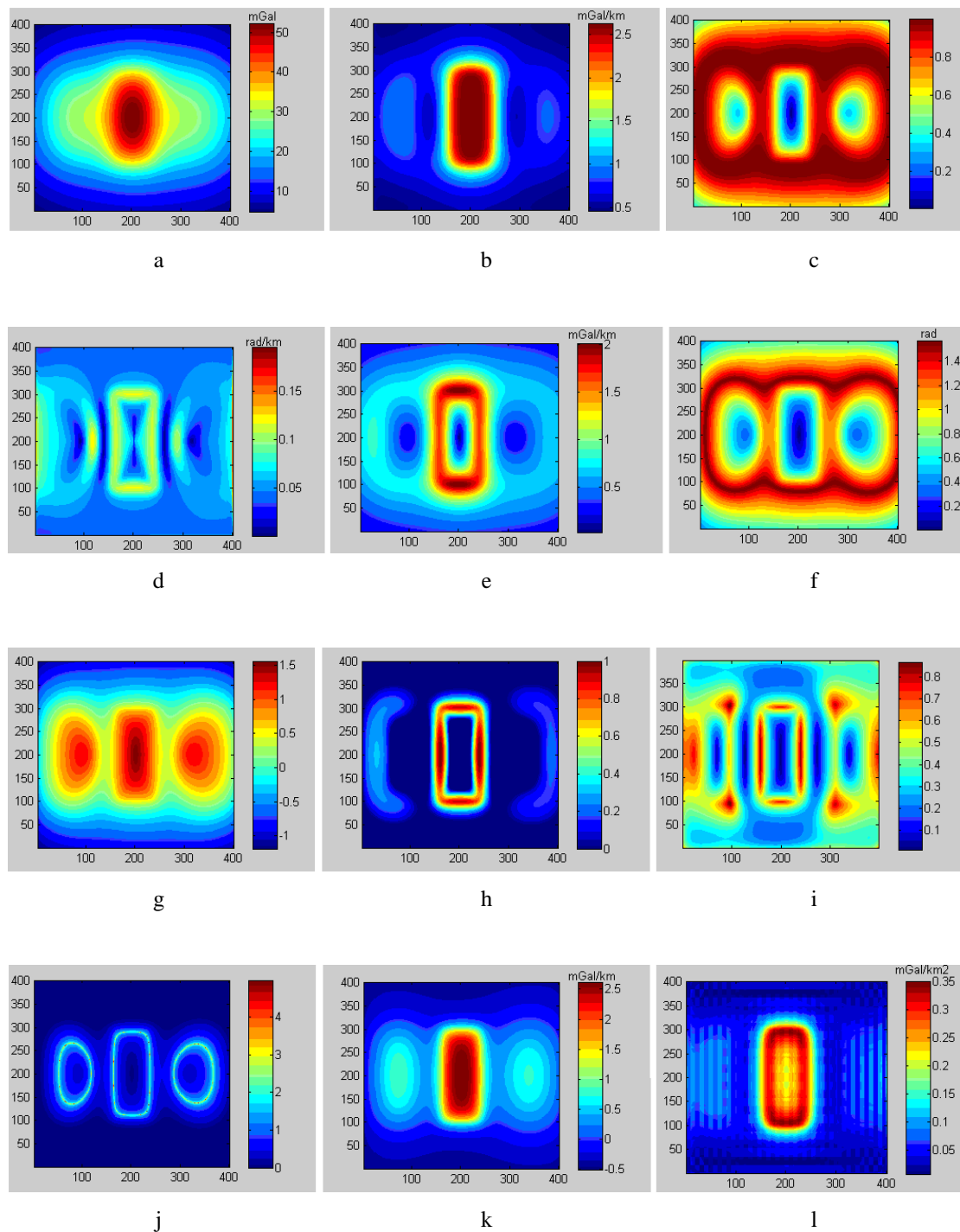
Figure 3. Plan views computed by applying various edge detection filters on the gravity anomaly of three vertical cubic models. a) Gravity anomaly, b) Analytic signal, c) Theta angle, d) Total horizontal derivative of tilt angle, e) Total horizontal derivative, f) Tilt angle, g) Normalized standard deviation, h) Normalised total horizontal gradient, i) Normalised first vertical derivative of total horizontal derivative, j) Hyperbolic of tilt angle, k) Vertical derivative, l) First vertical derivative of analytic signal

Figure 4. Geographical position of the study area

According to geological and stratigraphic studies (Figure 5), Dariyan, Kazhdumi, Sarvak, Ilam, Gurpi, Jahrum, Asmari and Gachsaran are the major geological formations in the study area. Dariyan formation is porous, locally vuggy and dolomitized. Limestone is the main lithology of this formation with low permeability. The formation ages backed to lower Cretaceous. Appropriate oil reservoirs are formed by the Albian aged (middle Cretaceous) Burgan formation. This formation is deltaic sandstones and characterized by high porosity and permeability. Shales and marls of the Kazhdumi formation seal the reservoirs both laterally and vertically. The entire area is covered by alluvial deposits. These deposits consist of sands and gravels which overlies the Marls (Agha Jari formation) and Gypsum (Gachsaran formation). Limestone of the Asmari formation underlies the Gachsaran formation. The outcrops of salts can be seen in the southern parts of the Gheshm Island and in some areas of northern seashores of the island including Poul, Gachin and Angoral salt plugs [18].
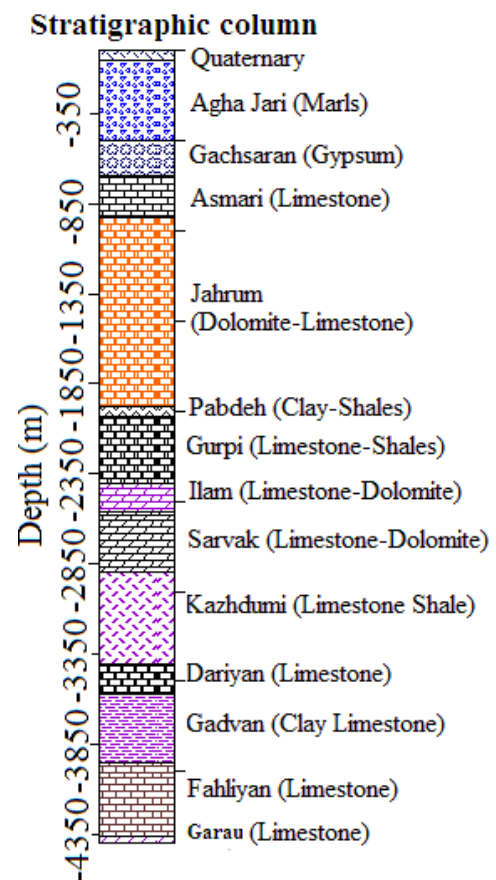

Figure 5. A simplified stratigraphic column of the study area

Figure 6a shows the Bouguer gravity anomaly map of the Gheshm area. Figure 6b shows the residual gravity anomaly map of the study area. The analytic signal, NSTD, THDR-TA and THDR of data, theta angle, tilt angle, TDX and HTA of data are shown in Figure 7. Almost all filters stand out a northeast-southwest structural trend.

The THDR better outlines the structural morphology and trend. It shows the salt plugs much better than other filters. Analytic signal and THDR successfully enhanced the edges of the shorter wavelength residual structures. NSTD, TDX and HTA filters highlighted the likely fault pattern and lineaments, with a dominant northeast-southwest structural trend.
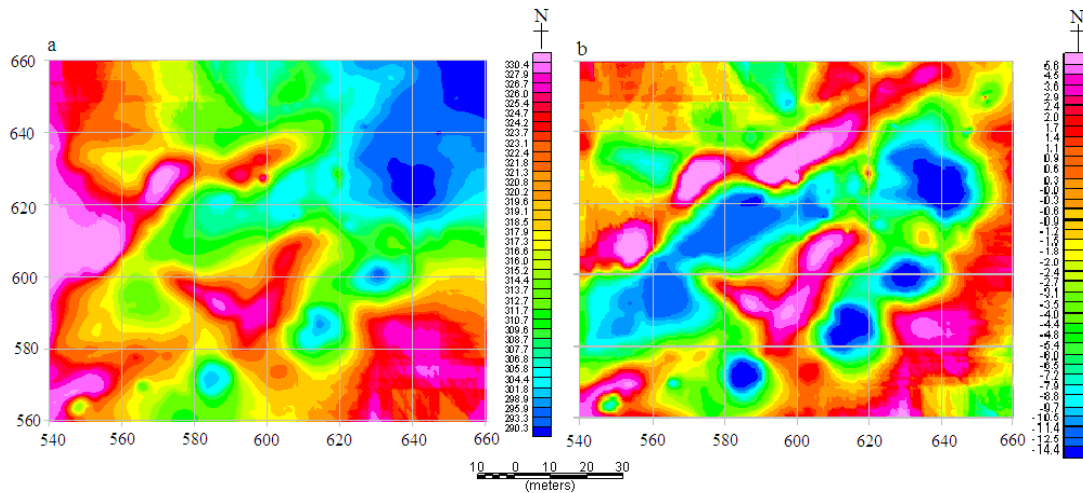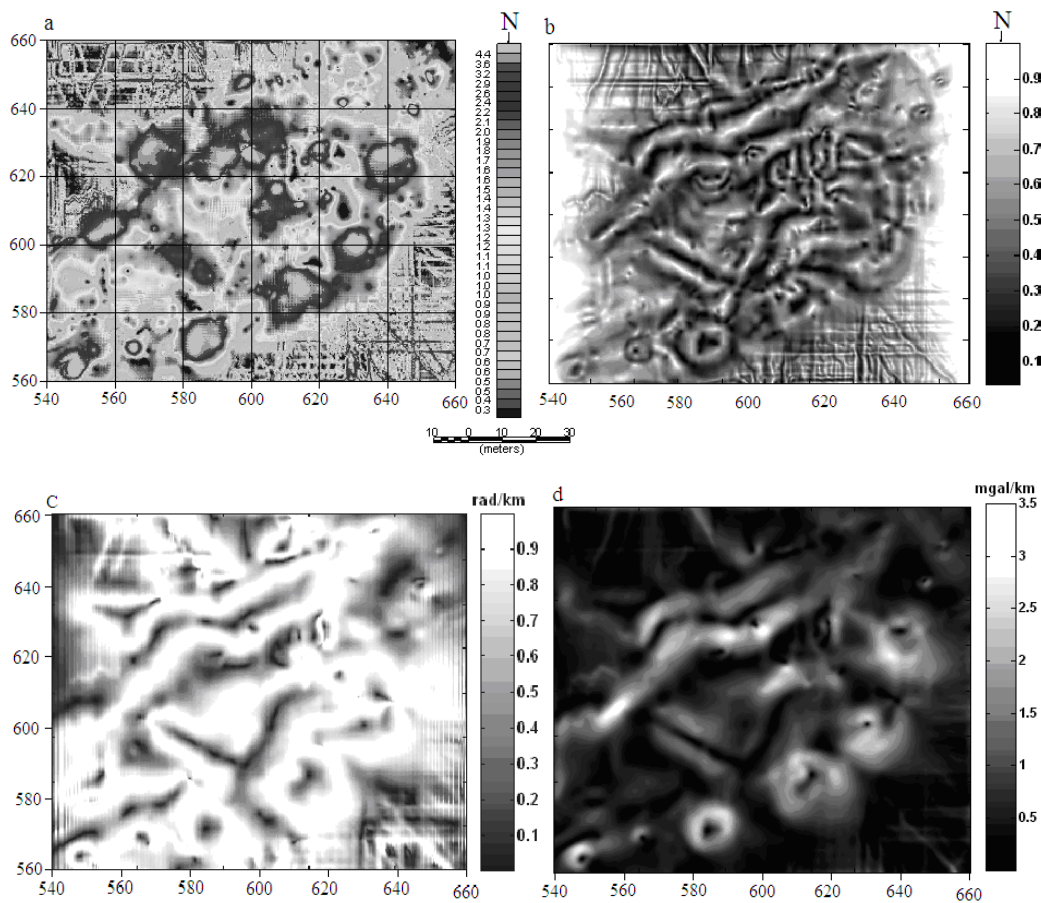

Figure 6. a) Bouguer gravity anomaly map of the Gheshm area, b) Residual gravity anomaly map computed by removing a second-order polynomial surface from the Bouguer gravity anomaly map
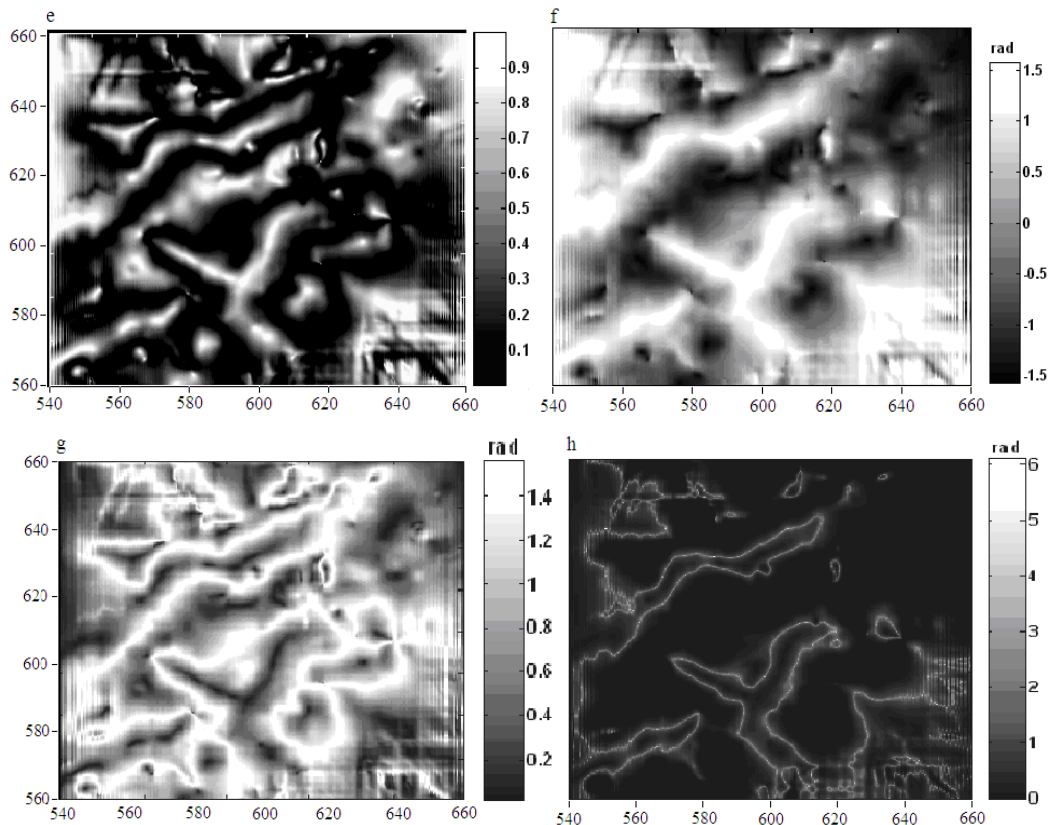
Figure 7. a) Analytic signal of the residual gravity map, b) NSTD of data, c) THDR-TA of data, d) THDR of data, e) Theta of data, f) Tilt of data, g) TDX of data, h) HTA of data

Conclusions

This paper presents the application of different edge detection methods to both synthetic and real gravity data in order to delineate the edges of subsurface structures. The capability of these filters decreased as the depth of sources increased. The application of the filters based on the derivative of local phase filters provided better response and acted as effective tool to delineate edges in gravity field data. The normalized standard deviation filter provided the best separation. Higher orders vertical derivatives made the interpretation more complicated, due to noise generation problem. The application of edge detection techniques on a real gravity data from the Gheshm sedimentary basin in the Persian Gulf in Iran showed that almost all filters exhibited a northeast-southwest structural trend. The THDR outlined the structural morphology and trend. It showed the salt plugs much better than other filters. Analytic signal and THDR successfully enhanced the edges of the shorter wavelength residual structures. NSTD, TDX and HTA filters highlighted the likely fault pattern and lineaments, with a dominant northeast-southwest structural trend. The results obtained from this study provide valuable information for geologists and petroleum engineers to delineate the horizontal location of salt plugs and indicate the buried faults, contacts and other tectonic and geological features.

References

[1] Oruç, B., Selim, H.H. (2011). Interpretation of magnetic data in the Sinop area of Mid Black Sea, Turkey, using tilt derivative, Euler deconvolution, and discrete wavelet transform. Journal of Applied Geophysics 74, 194− 204.

[2] Blakely, R.J., Simpson, W. (1986). Approximating edges of source bodies from magnetic or gravity anomalies. Geophysics 51, 1494− 1498.

[3] Cooper, G.R.J., Cowan, D.R. (2008). Edge enhancement of potential field-data using normalized statistics. Geophysics 73, H1-H4.

[4] Miller, H.G., Singh, V. (1994). Potential field tilt—a new concept for location of potential field sources. Journal of Applied Geophysics 32, 213− 217.

[5] Cordell, L., Grauch, V.J.S. (1985). Mapping basement magnetization zones from aeromagnetic data in the San Juan Basin, New Mexico. In: Hinze, W.J. (Ed.), The Utility of Regional Gravity and Magnetic Anomaly

Maps: Society of Exploration Geophysics, pp. 181− 197.

[6] Hansen, R.O., Pawlowski, R.S., Wang, X. (1987). Joint use of analytic signal and amplitude of horizontal gradient maxima for three-dimensional gravity data interpretation. 57th Annual International Management, Society of Exploration Geophysics, Expanded Abstracts 100–102.

[7] Thurston, J.B., Smith, R.S. (1997). Automatic conversion of magnetic data to depth, dip and susceptibility contrast using the SPI method. Geophysics 62, 807− 813.

[8] Boschetti, F. (2005). Improved edge detection and noise removal in gravity maps via the use of gravity gradients. Journal of Applied Geophysics 57, 213− 225.

[9] Wijns, C., Perez, C., Kowalczyk, P. (2005). Theta map: edge detection in magnetic data. Geophysics 70, 39–43.

[10] Fedi, M., Cella, F., Quarta, T., Villani, A.V. (2010). 2D continuous wavelet transform of potential fields due to extended source distributions. Applied and Computational Harmonic Analysis 28, 320− 337.

[11] Oruç, B. (2011). Edge detection and depth estimation using a tilt angle map from gravity gradient data of the Kozakl-Central Anatolia region, Turkey. Pure and Applied Geophysics 168, 1769–1780.

[12] Sertcelik, I., Kafadar, O. (2012). Application of edge detection to potential field data using eigenvalue analysis of structure tensor. Journal of Applied Geophysics 84, 86− 94.

[13] Ma, G., and Li, L. (2012). Edge detection in potential fields with the normalized total horizontal derivative. Computers & Geosciences 41, 83− 87.

[14] Verduzco, B., Fairhead, J.D., Green, C.M. (2004). New insights into magnetic derivatives for structural mapping. The Leading Edge 23 (2), 116− 119.

[15] Nabighian, M.N. (1984). Toward a three dimensional automatic interpretation of potential field data via generalized Hilbert transforms: Fundamental relations. Geophysics 49(6), 780-786.

[16] Cooper, G.R.J., Cowan, D.R. (2006). Enhancing potential field data using filters based on the local phase. Computers and Geosciences 32, 1585− 1591.

[17] Hadadian, A. (2011). Precise boundary detection of potential field anomalies using local phase filters, M.Sc. Thesis, Shahrood University of Technology, 102p.

[18] Hosseini, S.A.A., Doulati Ardejani, F., Tabatabaie, S.H., Hezarkhani, A. (2013). A three-dimensional multi-body inversion process of gravity fields of the Gheshm sedimentary basin. Arabian Journal for Science and Engineering (Accepted for publication, 27 October 2013).